academicJournals

Vol. 9(45), pp. 3369-3378, 6 November, 2014
DOI: 10.5897/AJAR2013.8008
Article Number: 34CD93A48442
ISSN 1991-637X

http://www.academicjournals.org/AJAR

African Journal of Agricultural Research

Full Length Research Paper

Assessment of soil salinity using electrical resistivity imaging and induced polarization methods

Ahzegbobor Philips Aizebeokhai

Department of Physics, College of Science and Technology, Covenant University, P. M. B. 1023, Ota, Ogun State, Nigeria.

Received 30 September, 2013; Accepted 10 October, 2014

2D imaging involving geoelectrical resistivity and time domain induced polarization has been used to assess the spatial variability of the physical properties of subsurface soil in Covenant University Farm, southwestern Nigeria. Apparent resistivity and chargeability of the induced polarization effect were concurrently measured along six traverses using Wenner array. The observed data were processed to produced 2D inverse models of the subsoil resistivity and chargeability. Soil samples were also collected and analysed for conductivity and salinity levels. The results show that the salinity level in the soil is within the range for normal soil and therefore healthy for plant growth. The inverse model sections were integrated with the laboratory test to qualitatively assess the salinity, degree of compaction, and thickness of the soil in the farm. Other petrophysical properties such as clay volume, moisture content and organic matter which are related to soil conductivity were also inferred. The study demonstrates that geoelectrical resistivity imaging can be a useful tool for effectively assessing the variations of soil condition in large tracts of land for precision agriculture.

Key words: Soil salinity, 2D imaging, geoelectrical resistivity, induced polarization, precision farming.

INTRODUCTION

The knowledge of soil properties is useful for agricultural practices and environmental impact analysis. Agricultural practice has always indicated that there are differences in the soil among nearby parcels of land; these differences are usually manifested in crops productivity. Many techniques have been used in determining subsurface soil properties, and their spatial and temporal variability. The distribution of these properties is often exploited in a more efficient way, allowing increased crops yield without necessarily using chemical fertilizers and pesticides (Robert, 2002; Rodriguez et al., 2010). Consequently, the environmental impacts on soils, surface water and groundwater due to agricultural activities can be considerably reduced. However, the mapping and characterization of soil properties as rapidly and accurately as possible can be very challenging. Geophysical techniques are effective, fast, and relatively inexpensive tools that can be used for rapid and accurate characterization of soil parameters. Geoelectrical resistivity survey is one of such geophysical methods that can be used to map and characterize the spatial and temporal variability of soil parameters (Williams and Baker, 1982; Mckenzie et al., 1989; Corwin and Lesch, 2003; Amezketa, 2007; Sudha et al., 2009). Geoelectrical

*Corresponding author. Email: a.p.aizebeokhai@gmail.com, philips.aizebeokhai@covenantuniversity.edu.ng.

resistivity survey makes use of the variations in the electrical properties of rocks and minerals in the subsurface.

Soil conductivity (or its inverse, resistivity) is influenced by a variety of factors including the salinity, clay volume, moisture content, porosity, mineralogy, organic matter and temperature of the soil. Thus, soil conductivity is a complex physiochemical property that results from the inter-relationship and interaction of these soil properties. Geoelectrical resistivity measurements can be used to assess the spatial distribution and temporal variability of any or a combination of these properties. Soil conductivity has been used to map and characterize spatial distribution of soil salinity (or total solute concentration) and assess other soil properties such as clay content, porosity and Cation Exchange Capacity (CEC) (Shevnin et al., 2006, 2007) which correlate well with conductivity.

Soil salinity is basically the amount of major dissolved inorganic solute present in the soil aqueous phase, which consists of soluble and readily dissolvable salts. These include charged species such as Na^+, K^+, Mg^{2+}, Ca^{2+}, Cl^-, HCO_3^-, NO_3^-, SO_4^{-2} and CO_3^2, non-ionic solutes, and ions that can combine to form pairs of ions (Corwin and Lesch, 2003). Soil salinity tends to increase over time due to various factors which are either natural or artificial. The natural factors include processes such as mineral weathering and saline water intrusion, while the artificial factors include practices such as irrigation, application of fertilizers and other anthropogenic activities. Soil salinity has been shown to have detrimental effect on plant growth; this effect is usually manifested in loss of stand, reduced and thwarted plant growth, and reduced yield and crop failure (Rhoades and Corwin, 1990; Rhoades and Loveday, 1990). Plant growth is important to humans and the ecosystems as plants serve a lot of purposes including food supply, protection of soil from erosion, prevention of desertification, provision of oxygen for respiration, and the reduction of carbon dioxide in the atmosphere through photosynthesis.

Soil salinity limits the amount of water and nutrients uptakes by plants from the soil by significantly reducing the osmotic potential, thus making it difficult for plants to extract water from the soil. Consequently, this results in low yield or complete destruction of the plants (Corwin and Lesch, 2003). Soils salinity may cause specific ion-toxicity thereby upsetting the nutritional balance of plants. Also, the salt composition of the soil water influences the composition of the cations on the exchange complex of the soil particles and consequently influences soil permeability. Apart from limiting crops yield and adversely affecting soil hydraulic parameters, soil salinity can negatively impact groundwater system as well as causing damages to infrastructures in the area through corrosion.

Different methods have been used for the assessment of soil salinity. Traditionally, soil salinity is assessed by visual crop observation. This traditional technique of visual crop observation is fast and economic; but its major disadvantage is that the plants would have been damaged or low yield would have been recorded before salinity is detected. Geophysical techniques can be used to detect or monitor salinity and other soil properties before having detrimental effects on plants (Rhoades et al., 1990, 1999). Soil salinity is commonly quantified in terms of the total concentration of dissolved soluble salts as measured by the electrical conductivity of the solution in dSm^{-1} (Corwin and Lesch, 2003). For a pure solution, the electrical conductivity σ_w is a function of the chemical composition and is characterized by the relation

$$\sigma_w = k\sum_{i=1}^{n} \lambda_i M_i |v_i|, \quad (1)$$

where k is the cell constant which accounts for the geometric factor of the electrodes, λ is the molar limiting ion conductivity ($S\,m^2\,mol^{-1}$), M is the molar concentration ($mol\,m^{-3}$), v is the absolute value of the ion charge, and i is the ion species in the solution. In practice, soil conductivity is determined for an aqueous extract of a soil sample.

In this study, electrical resistivity and time domain induced polarization geophysical techniques together with laboratory analysis were used to map and characterize the resistivity and chargeability of the subsurface soil in Covenant University Farm. Most part of the farm is usually water logged during the raining season due to underlying relatively impermeable near-surface lateritic clay layer. This is expected to lead to increased soil salinization in the area. The soil samples collected were analysed for conductivity and salinity. Similarly, the inverse model sections of the observed apparent resistivity and chargeability were used to assess the salinity level, degree of compaction, as well as the thickness of the soil. Other petrophysical properties including clay volume, moisture content and organic matter which are related to soil conductivity are inferred from the resistivity models and laboratory results. This is because the ionic charges in the salts can significantly affect the flow of electric current in the soil.

SITE DISCRIPTION AND GEOLOGICAL SETTING

The study site (Covenant University Farm, Lat. 6.67° N and Long. 3.16° E) is located in the eastern part of the Dahomey Basin, southwestern Nigeria. The basin is a combination of inland, coastal and offshore basins, and stretches along the continental margin of the Gulf of Guinea (Figures 1 and 2). The area is generally gently sloping low-lying and is characterized by two main

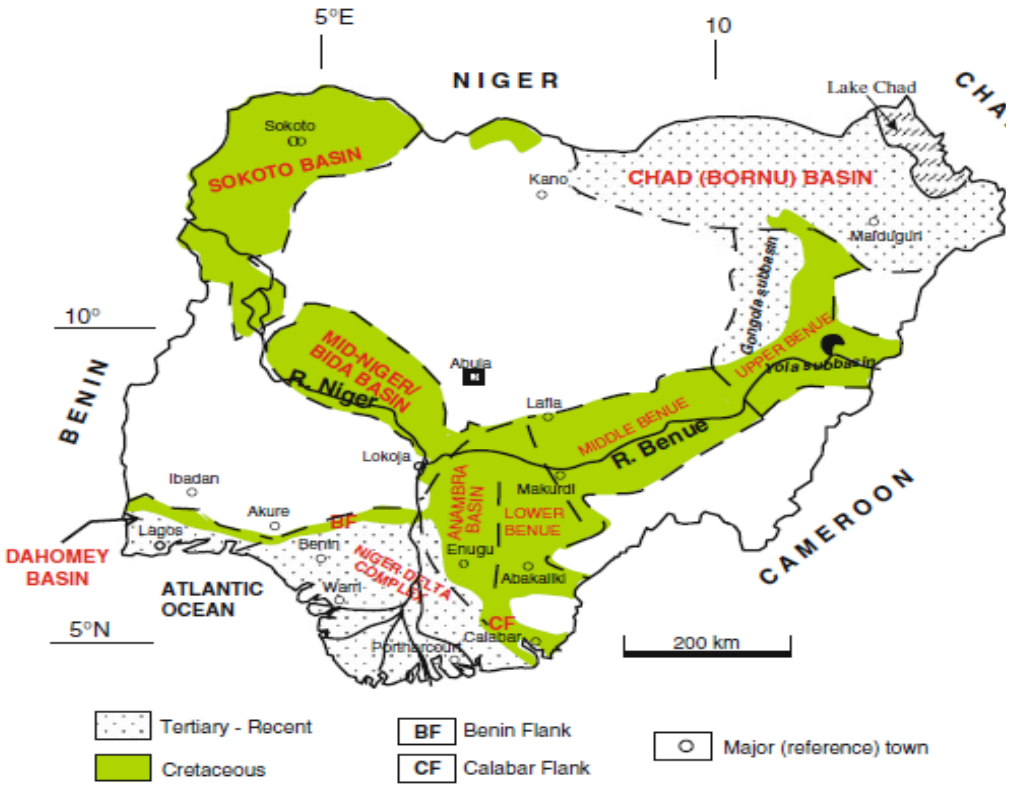

Figure 1. Geological map of Nigeria showing the major geological components: Basement, Younger Granites, and Sedimentary Basins (after Obaje, 2009).

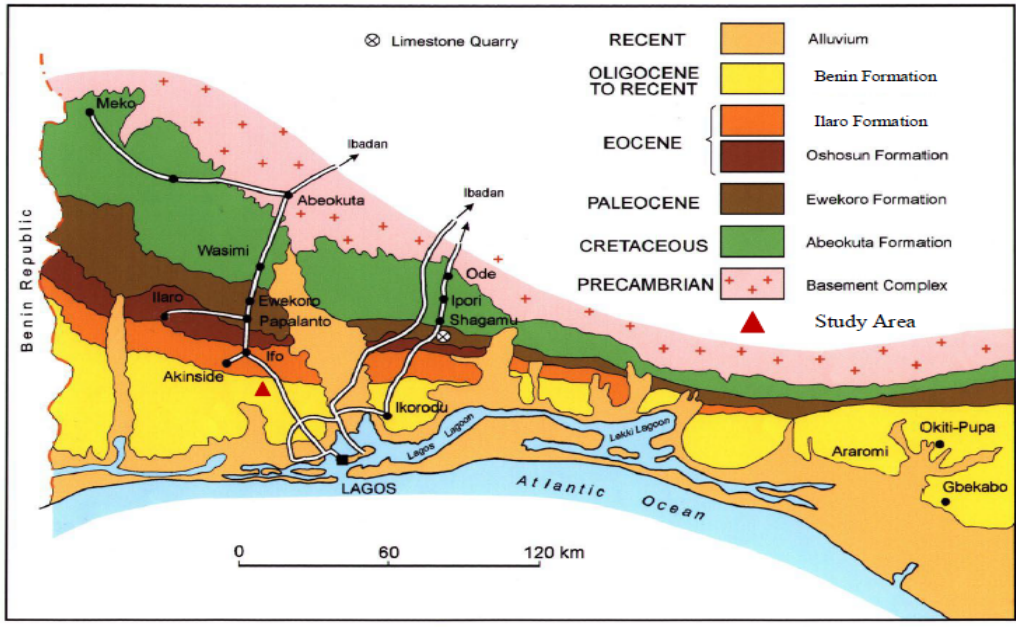

Figure 2. Geological map of the Nigerian part of the Dahomey embayment (modified after Gebhardt et al., 2010).

climatic seasons – the dry season that spans from November to March and raining (or wet) season between April and October. Occasional rainfalls are often witnessed within the dry season due to its proximity to the

Atlantic Ocean. Rainfall forms the major source of groundwater recharge in the area; mean annual rainfall is greater than 2000 mm. The mean monthly temperature ranges from 23°C in July to 32°C in February. Because of its proximity to the coast, the area is under the influx of sea salt and other types of aerosols sprayed from the Atlantic Ocean; this can potentially increase the salinity of the subsoil.

The rocks in the basin are Late Cretaceous to Early Tertiary in age (Jones and Hockey, 1964; Ogbe, 1970; Omatsola and Adegoke, 1981; Okosun, 1990; Billman, 1992; Olabode, 2006). The stratigraphy of the basin has been grouped into six lithostratigraphic formations namely, from oldest to youngest, Abeokuta, Ewekoro, Akinbo, Oshosun, Ilaro and Benin Formations. However, some workers have described the Cretaceous Abeokuta Formation as Abeokuta Group consisting of Ise, Afowo and Araromi Formations (Omatsola and Adegoke, 1981). The Cretaceous Abeokuta Formation mainly composed of poorly sorted sequence of continental grits and pebbly sands over the entire basin with occasional siltstones, mudstones, shale-clay with thin limestone beds due to marine transgression. Overlying the Abeokuta Formation is the Ewekoro Formation which is predominantly composed of shallow marine limestone due to the contamination of the marine transgression. The Ewekoro limestones are Palaeocene in age. The Ewekoro Formation is overlain by the shale-dominated Akinbo Formation of Late Palaeocene to Early Eocene (Ogbe, 1970; Okosun, 1990). The Akinbo Formation is overlain by the Oshosun Formation which composed of Eocene shale and then Ilaro Formation which is predominantly a sequence of coarse sandy estuarine, deltaic and continental beds; the Ilaro Formation is characterized with rapid lateral facies changes. Overlying the Ilaro Formation is the Benin Formation which is predominantly coastal plain sands and Tertiary alluvium deposits.

The local geology is consistent with the regional geology and is predominantly Coastal Plain Sands and Recent sediments. The Coastal Plain sands consists of poorly sorted clayey sand, reddish mud/mudstone, clay lenses, sandy clay with lignite of Miocene to Recent underlain by a sequence of coarse sandy estuarine, deltaic and continental beds characterised by rapid changes in facies. The top soil is mainly sandy loam which is rich in organic matter and underlain by unconsolidated sand with varying thickness ranging from about 1.0 to 2.5 m across the farm land. This unconsolidated sand is underlain by more consolidated and relatively impermeable lateritic clay unit. This causes runoff water to settle in most parts of the area after rainfall for periods ranging from few days to weeks. At the time of this study, the farm land has been tilled and cultivated with maize and plantain already growing on it. Organic fertilizer was applied on the farm. The aquifer system is confined and relatively deep with depth ranging from about 45 m to >65 m as characterized from previous studies (Aizebeokhai and Oyebanjo, 2013; Aizebeokhai and Oyeyemi, 2014).

METHODOLOGY

Laboratory measurements

A total of twelve soil samples were collected from the study site and analyzed in laboratory. The samples were collected from two locations, at 20 m and 70 m marks, on each profile except for Traverses 5 and 6 where the samples were collected at 20 m and 50 m. The soil samples were limited to the top soil within 15 cm range. The samples were visually observed so as to determine their physical characteristics which can be used as aids to grain size identification. The samples were dried to remove the moisture content left in the soil samples. During the laboratory testing, distilled water was used in every step that involved liquid. The beakers, measuring cylinders and spatulas were washed with distilled water and oven dried so as to remove traces of ions and water molecules present in the apparatus. A small amount of each sample collected, approximately 2 g, was placed in the beakers and 100 ml of distilled water was added to it. The mixture was then stirred properly to accelerate the dissolving of the traces of salt present in the samples. The solutions were covered and left for about 70 h so that any salt present in the soil samples could dissolve properly.

The conductivity meter was calibrated using two solutions 1413 and 848 µsKm, respectively so as to sterilize the sensing part of the conductivity meter. The JENWAY 4510 conductivity meter, which applies an alternating current (I) at a specified frequency to two active electrodes and measures the potential (V) was used for determining the conductance. The conductivity meter then uses the conductance and cell constant to determine the conductivity displayed. The current source was adjusted so that the measured potential (V) equals the reference potential (approximately ± 200 mV). The HANNA salinity meter was used to measure the salinity level in the samples. The temperature of the samples was also determined. The conductivity and salinity meters were re-calibrated after each reading before using it for the next sample. The conductivity of the samples was measured in micro-Siemens per meter (µS/m) and converted to deci-Siemens per meter (dS/m) and the salinity levels are expressed in percentage.

Geophysical survey

Six 2D geoelectrical resistivity and time domain induced polarization profiles were conducted with the aid of ABEM Terrameter (SAS 1000/4000 series). Traverses 1 to 4 were 100 m in length, while Traverses 5 and 6 were 70 m and 80 m in length respectively due to limitation of space. The 2D traverses were conducted in the west-east direction and are separated from each other with a distance of 15 m. Wenner electrode configuration with minimum electrode spacing of 1.0 m was used for the data measurements, and a data level of 5 (maximum electrode spacing of 5.0 m) was achieved in each of the profiles. The minimum electrode spacing and data level reached ensures that the effective depth of investigation is confined to the root zone (about 2.0 m depth). Care was taken to minimize electrode positioning error in the measurements throughout the survey. To ensure quality and minimized error in the data collection, the measurements were stacked for each observation and the data stacking range between 3 and 6. The root-mean-squares error in the measurement was generally less than 0.3%. Data measurements with root-mean-squares error up to 0.5% or higher were repeated, after ensuring that the electrodes were in good contact with the ground. The apparent resistivity and apparent

Table 1. Conductivity and salinity level from laboratory observations.

Samples	Temperature (°C)	Weight (g)	Conductivity (dS/m)	Salinity (%)
T_1 (20 m)	28.0	2.0037	6.2×10^{-4}	0.5
T_1 (70 m)	28.0	2.0057	1.085×10^{-4}	0.2
T_2 (20 m)	28.0	2.0023	1.156×10^{-4}	0.2
T_2 (70 m)	27.9	2.0041	2.41×10^{-4}	0.2
T_2 (20 m)	27.9	2.0003	7.80×10^{-5}	0.2
T_3 (70m)	28.1	2.0054	1.069×10^{-4}	0.2
T_4 (20m)	28.1	2.0058	7.12×10^{-5}	0.5
T_4 (70m)	28.0	2.0068	1.243×10^{-4}	0.2
T_5 (20m)	28.0	2.0047	1.106×10^{-4}	0.4
T_5 (50m)	27.8	2.0057	8.11×10^{-5}	0.3
T_6 (20m)	27.8	2.0680	8.40×10^{-5}	0.4
T_6 (50m)	27.8	2.0467	1.649×10^{-4}	0.4

Table 2. Standard salinity level for soil (Richards, 1954).

Electrical conductivity (dS/m)	Interpretation	Inference
0 – 2	Normal soil	Little or no effect on growth of plant
2 – 4	Saline	Affects only very sensitive plants
4 – 8	Slightly saline	Affects many plants
8 – 16	Moderately saline	Affect tolerant plants
> 16	Severely saline	Affects even very tolerant plants

chargeability were measured concurrently. The chargeability of IP effect was measured by integrating the area under the IP decay curve according to the relation

$$M = \frac{1}{V_0}\int_{t_1}^{t_2} V(t)dt\,, \tag{2}$$

where V_0 is the voltage measured before the current is turned off, t_1 and t_2 is the start and stop time interval respectively, and $V(t)$ is the decaying voltage.

The observed apparent resistivity and chargeability data sets for each of the 2D profiles were processed with RES2DINV computer code (Loke and Barker, 1996). The RES2DINV computer program uses a nonlinear optimization technique which automatically determines a 2D resistivity model of the subsurface for the input apparent resistivity data (Griffiths and Barker, 1993; Loke and Barker, 1996). The program divides the subsurface into a number of rectangular blocks according to the spread of the observed data. Least-squares inversion with standard least-squares constraint which attempt to minimize the square of the difference between the observed and the calculated apparent resistivity values was used to invert all the 2D traverses. Smoothness constraint was applied to the model perturbation vector only and appropriate damping factors were selected. Apparent resistivity datum points with greater than 50% RMS errors were eliminated from the 2D data set before the final inversion.

RESULTS AND DISCUSSION

The JENWAY conductivity meter and HANNA salinity meter were used to measure the conductivity and salinity level for each sample solution, respectively. The salinity levels obtained are given in percentages. Similarly, the conductivity values were measured in micro-Siemens per meter (μS/m) and converted to deci-Siemens per meter (dS/m). The observed salinity level and conductivity in soil samples are presented in Table 1. The standard values for salinity levels in soils are presented in Table 2 (Richards, 1954). The laboratory observations showed that the conductivities and salinity levels of the soil were generally low and within the limit for normal soil for plant growth.

The inverse resistivity and chargeability models obtained from the data inversion are presented in Figures 3 to 8. The inverse model resistivity and chargeability sections presented were achieved after the fifth iteration, except for Traverse 2 which converges after the third iteration. The effective depth of investigation for the model sections is about 2.8 m. The root-mean-squares errors observed in the inverse resistivity models range between 4.2 and 7.2%. Correlation between measured chargeability data and calculated ones shows low noise in IP data. The root-mean-squares errors observed in the chargeability inverse models are much lower than those of the resistivity inverse models, and range from 0.11 to 0.29%.

The tilled layer is largely characterized with very low resistivity values and can thus be easily discriminated from the more compacted region. The inverse resistivity

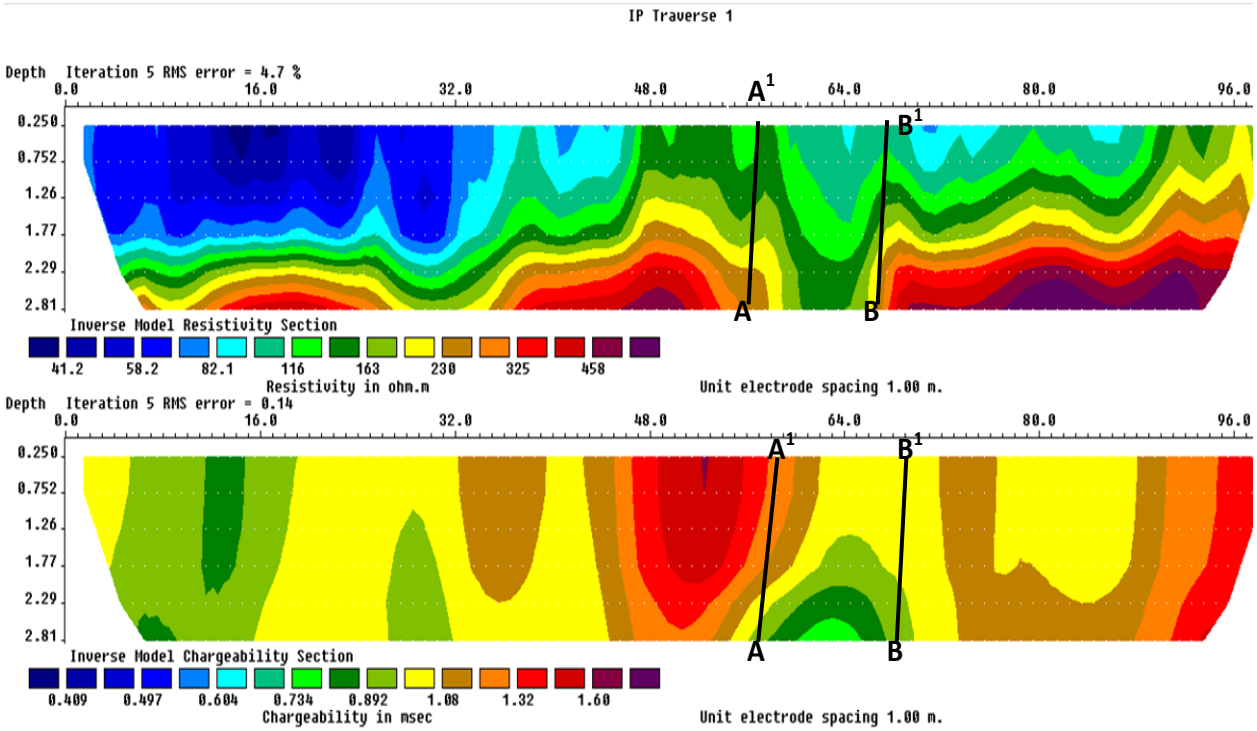

Figure 3. Inverse resistivity and chargeability model sections for Traverse 1.

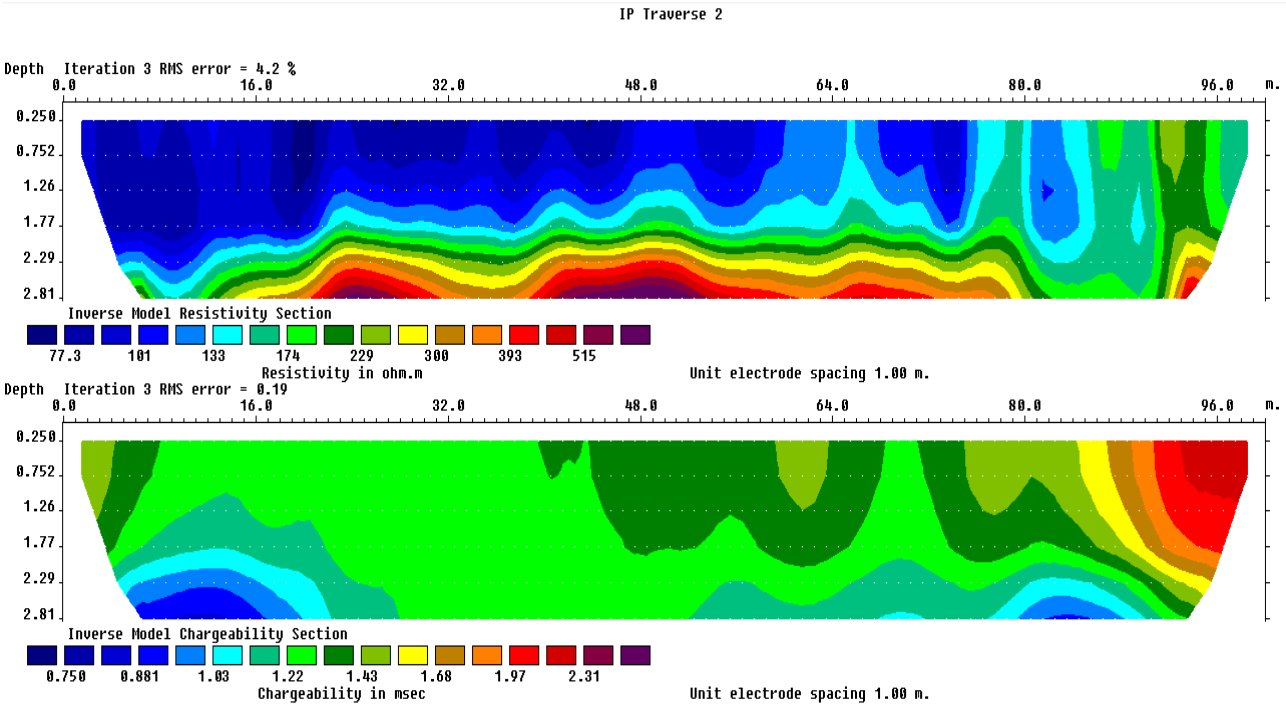

Figure 4. Inverse resistivity and chargeability model sections for Traverse 2.

models are generally characterized with low resistivity values in all the traverses, ranging from about 40 to 700 $\Omega\, m$. Low resistivity (<$100\ \Omega m$) values are particularly pronounced in the west end of the farm. On the whole,

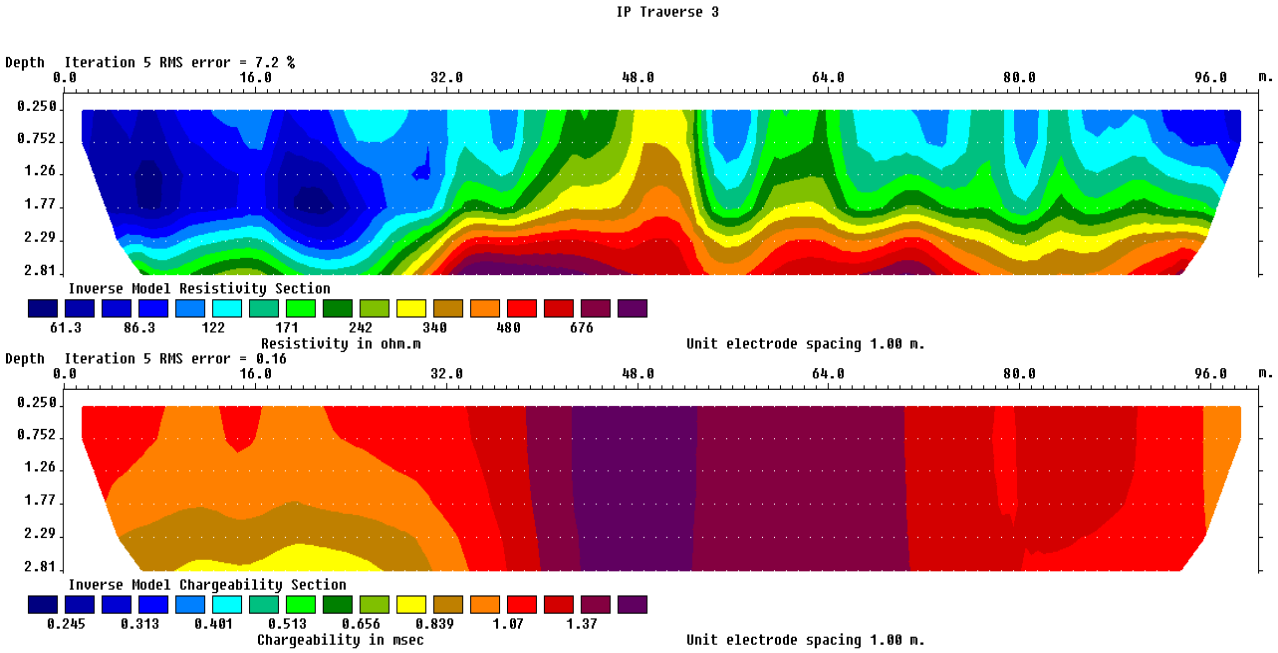

Figure 5. Inverse resistivity and chargeability model sections for Traverse 3.

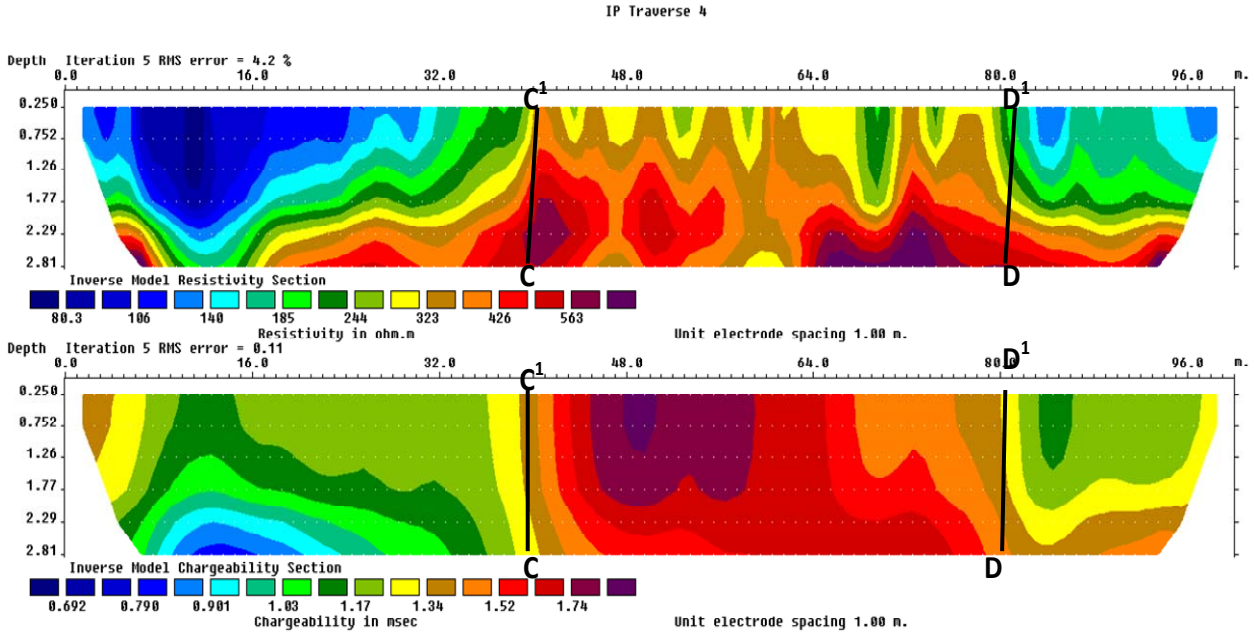

Figure 6. Inverse resistivity and chargeability model sections for Traverse 4.

the inverse model resistivity is averagely less than $100\Omega m$ to an average model depth of about 2.2 m, indicating high moisture content (and/or clay mineral) and less consolidated soil within this depth. However, relatively higher model resistivity values are observed in Traverse 4. Field observation shows that the subsoil in this area is more compacted than most parts of the survey farm. This indicates that the subsoil in the study site is generally conductive.

Soil moisture, porosity, degree of consolidation and organic matter are thought to be the dominant factors that determine the observed inverse model resistivity. Areas

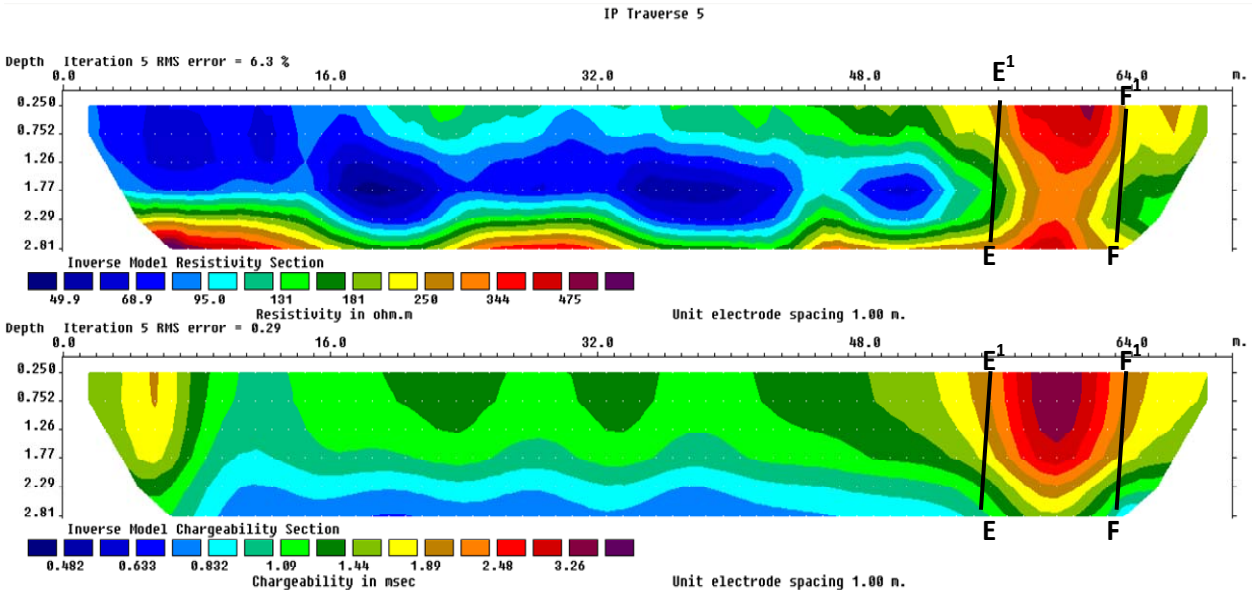

Figure 7. Inverse resistivity and chargeability model sections for Traverse 5.

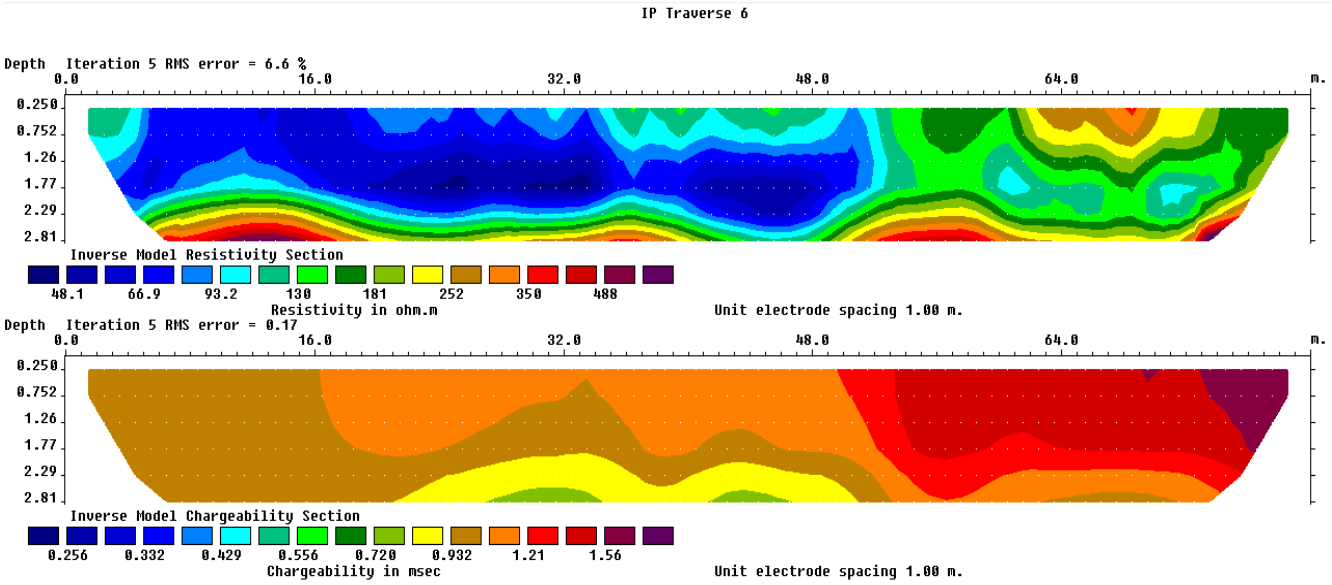

Figure 8. Inverse resistivity and chargeability model sections for Traverse 6.

with loosed soil are generally more porous and contain higher soil moisture content. Low resistivity anomalies ($<100\,\Omega m$) were generally observed in these areas. Although, soil salinity could significantly decrease model resistivity values, the observed low resistivity values in the inverse model sections are not attributed to soil salinity. Results from the laboratory test, indicating low salinity level in the sub soil, further confirmed that the impact of salinity in the observed model resistivity is minimal.

The model chargeability observed in the inverse model sections is generally low, ranging from 0.4 to 3.5 ms. Strong correlations are observed between the resistivity and chargeability anomalies in the inverse model sections for Traverses 2, 5 and 6 with high resistivity values corresponding to relatively low chargeability values. Areas with relatively high resistivity anomalies ($>100\,\Omega m$) are thought to be regions with more consolidated soil materials, consisting mainly of lateritic soil. However, some anomalies with high resistivity values also produced high chargeability values; for example, anomaly marked CC^1 and DD^1 in Traverse 4

and that marked EE^1 and FF^1 in Traverse 5. The anomaly marked AA^1 and BB^1 in the inverse model section for Traverse 1 is thought to be a fractured zone which serves as conduit path for fluid flow.

The chargeability of a given medium is a measure of the discharge of the polarization in the medium. Thus, it is related to the permittivity and resistivity of the subsurface materials as well as the porosity and moisture/water content in the subsurface media. Other factors that can significantly influence the chargeability of surface materials are grain size and shape of the constituent particles, mineral volume fraction and mineral conductivity. Strong IP effects are commonly observed in sediments containing clays disseminated on the surface of larger grains. Hence, clayey sand and clayey sandstone typically displays large IP effects. In contrast, compacted clays are usually associated with low IP effects, as the ohmic conduction dominates current flow. Small measurable IP effects are associated with clean sand and gravel (Vanhala, 1997).

The model sections generally shows low chargeability ranging from 0.4 to 3.5 ms. This indicates that the soils are mainly composed of sandy materials and less disseminated clayey materials. A careful analysis of the resistivity and chargeability in the inverse model sections show that observed low resistivity anomalies did not show distinct and relatively high chargeability anomalies. Thus, the observed low resistivity anomalies are not principally due to increased clay volume in the subsoil. This is because clay is expected to produce high chargeability anomaly due to cationic exchange capacity. Hence, the observed low resistivity anomaly is mainly due to increased porosity and high moisture content in the subsoil.

Conclusions

The knowledge of the spatial distribution of soil petrophysical properties is useful for precision agriculture as well as environmental impact analysis. In this study, apparent resistivity and chargeability of the subsoil were concurrently measured along six traverses using Wenner electrode configuration. 2D images of the inverse models of geoelectrical resistivity and chargeability of the induced polarization effects of the area investigated are produced. The 2D model sections of the geoelectrical resistivity and chargeability were used to qualitatively assess the spatial variability of the salinity, degree of compaction, and horizontal thickness of the subsoil. Other soil properties including clay volume, moisture content and organic matter, which are related to the conductivity, were equally inferred from the inverse model sections. Soil samples analysed for conductivity and salinity showed that the salinity level in the study area is within range for normal soil and therefore healthy for plant growth. Consequently, the low resistivities observed in the inverse model sections are not attributed to increased salinization in the soil but due principally to the effect of tillage, moisture content and presence of organic matter in the soil. The study demonstrates that geoelectrical resistivity imaging can be effectively used to map and assess the saptial variability of soil properties in large tracts of land for precision agricultures and environmental impact analysis. The degree of relaibility of the subsoil resistivity model can be significantly improved if the technique is combined with other geophysical methods such as self potential, induced potential and electromagnetic methods, which are equally sensitive to these petrophysical parameters.

Conflict of Interest

The author(s) have not declared any conflict of interests.

REFERENCES

Aizebeokhai AP, Oyebanjo OA (2013). Application of vertical electrical soundings to characterize aquifer potential in Ota, Southwestern Nigeria. Int. J. Phys. Sci. 8(46):2077-2085.

Aizebeokhai AP, Oyeyemi KD (2014). Application of Geoelectrical Resistivity Imaging and VLF-EM for Subsurface Characterization in a Sedimentary Terrain, Southwestern Nigeria. Arabian J. Geosci. DOI: 10.1007/s12517-014-1482-z.

Amezketa E (2007). Soil salinity assessment using direct soil sampling from a geophysical survey with electromagnetic technology: A case study. Spanish J. Agric. Res. 5(1):91-101. http://dx.doi.org/10.5424/sjar/2007051-225

Billman HG (1992). Offshore stratigraphy and Paleontology of Dahomey (Benin) Embayment. NAPE Bull. 70(02):121-130.

Corwin DL, Lesch SM (2003). Application of soil electrical conductivity to precision agriculture: theory, principles and guidelines. Agron. J. 95(3):455-471. http://dx.doi.org/10.2134/agronj2003.0455

Gebhardt H, Adekeye OA, Akande SO (2010). Late Paleocene to initial Eocene thermal maximum foraminifera biostratigarphy and paleoecology of the Dahomey Basin, southwestern Nigeria. Gjahrbuch Der Geologischem Bundesantalt 150:407-419.

Griffiths DH, Barker RD (1993). Two dimensional resistivity imaging and modelling in areas of complex geology. J. Appl. Geophys. 29:211-226. http://dx.doi.org/10.1016/0926-9851(93)90005-J

Jones HA, Hockey RD (1864). The geology of part of southwestern Nigeria. Geol. Survey Nig. Bull. 31:101.

Loke MH, Barker RD (1996). Practical techniques for 3D resistivity surveys and data inversion. Geophys. Prospect. 44:499-524. http://dx.doi.org/10.1111/j.1365-2478.1996.tb00162.x

McKenzie RC, Chomistek W, Clark NF (1989). Conversion of electromagnetic induction readings to saturated paste extracts values in soils for different temperature, texture, and moisture conditions. Can. J. Soil Sci. 69:25-32. http://dx.doi.org/10.4141/cjss89-003

Obaje NG (2009). Geology and mineral resources of Nigeria. In: Brooklyn SB, Bonn HJN, Gottingen JR, Graz KS (ed), Lecture Notes in Earth Sciences, Springer. http://dx.doi.org/10.1007/978-3-540-92685-6

Ogbe FAG (1970). Stratigraphy of strata exposed in the Ewekoro quary, Western Nigeria. In: Dessauvagie TFJ, Whiteman AJ (ed), *African Geology*, University of Ibadan Press, Nigeria. pp. 305-324.

Okosun EA (1990). A review of the Cretaceous stratigraphy of the Dahomey Embayment, West Africa. Cretaceous Res. 11:17-27. http://dx.doi.org/10.1016/S0195-6671(05)80040-0

Olabode SO (2006). Siliciclastic slope deposits from the Cretaceous Abeokuta Group, Dahomey (Benin) Basin, southwestern Nigeria. J. Afr. Earth Sci. 46:187-200. http://dx.doi.org/10.1016/j.jafrearsci.2006.04.008

Omatsola ME, Adegoke OS (1981). Tectonic evolution and Cretaceous stratigraphy of the Dahomey Basin. Nig. J. Min. Geol. 18(01):130-

137.
Rhoades JD, Corwin DL (1990). Soil electrical conductivity: Effects of soil properties and application to soil salinity appraisal. Commun. Soil Sci. Plant Anal. 21:837-860. http://dx.doi.org/10.1080/00103629009368274
Rhoades JD, Corwin DL, Lesch SM (1999). Geospatial measurements of soil electrical conductivity to assess soil salinity and diffuse salt loading from irrigation. In: Corwin DL, Loague K, Ellsworth TR (Eds.) Assessment of Non-point Source Pollution in the Vadose Zone. Geophysical Monograph 108, American Geophysical Union, pp. 197-215.
Rhoades JD, Loveday J (1990). Salinity in irrigated agriculture. In: Stewart BJ, Nielsen DR (Eds.) Irrigation of Agricultural Crops. Agronomy Monograph 30, ASA, CSSA and SSSA, Madison WI, pp. 1089-1142.
Rhoades JD, Shouse PJ, Alves WJ, Manteghi MN, Lesch SM (1990). Determining soil salinity from soil electrical conductivity using different models and estimates. Soil Sci. Soc. Am. J. 54:46-54.
Richards LA (1954). Diagnosis and improvement of saline and alkali soils. U.S. Department of Agriculture (U.S.D.A) Agricultural Handbook, Washington DC: P. 60.
Robert PC (2002). Precision agriculture: a challenge for crop nutrition management. Plant Soil, 247:143-149. http://dx.doi.org/10.1023/A:1021550219371
Rodriguez OD, Torres MLG, Shevnin V, Ryjov A (2010). Estimation of soil petrophysical parameters based on electrical resistivity values obtained from lab and in-field electrical measurements. Geophys. J. Int. 51(1):5-15.
Shevnin V, Rodriguez OD, Mousatov A, Hennandez DF, Martinez Z, Ryjov A (2006). Estimation of soil petrophysical parameters from resistivity data: Application to oil contamination site characterization. Geophys. J. Int. 45(3):179-193. http://dx.doi.org/10.1111/j.1365-2478.2007.00599.x
Shevnin V, Mousatov A, Ryjov A, Delgado-Rodríguez O (2007). Estimation of clay content in soil based on resistivity modeling and laboratory measurements. Geophys. Prospect. 55:265-275.
Sudha K, Israil M. Mittal S, Rail J (2009). Soil characterization using electrical resistivity tomography and geotechnical investigations. J. Appl. Geophys. 67:74-79. http://dx.doi.org/10.1016/j.jappgeo.2008.09.012
Vanhala H (1997). Mapping oil-contaminated sand and till with the spectral induced polarization (SIP) method. Geophys. Prospect. 45:303-326. http://dx.doi.org/10.1046/j.1365-2478.1997.00338.x
Williams BG, Baker GC (1982). An electromagnetic induction technique for reconnaissance surveys of soil salinity hazards. Aust. J. Soil Res. 20:107-118. http://dx.doi.org/10.1071/SR9820107